

Correlation for the Sauter Mean Diameter of a Prefilmer Airblast Atomizer at Varying Operating Conditions

Melanie Volz*, Peter Habisreuther, and Nikolaos Zarzalis

DOI: 10.1002/cite.201600007

© 2016 The Authors. Published by Wiley-VCH Verlag GmbH & Co. KGaA. This is an open access article under the terms of the Creative Commons Attribution-NonCommercial-NoDerivs License, which permits use and distribution in any medium, provided the original work is properly cited, the use is non-commercial and no modifications or adaptations are made.

One of the key factors that affect the combustion performance in gas turbines and therefore the amount of pollutant emission and the efficiency is the atomization quality of the liquid fuel. Often reliable droplet size distributions for combustion simulations are missing. In this work a correlation for the Sauter mean diameter based on energy equilibrium is derived and compared to results from three-dimensional numerical simulation of the atomization of a liquid film and to an empirical correlation from the literature. It is shown that the derived correlation agrees better with the results of the simulations than the empirical correlation.

Keywords: Mean film thickness, Prefilmer airblast atomizer, Sauter mean diameter, Shear flow, Surface stripping, Volume of fluid method

Received: February 02, 2016; *revised:* May 31, 2016; *accepted:* August 16, 2016

1 Introduction

The more stringent requirements in the design of combustion systems for aero engine applications to enhance efficiency and to lower pollutant emissions require, amongst others, the optimization of the injection system [1] as the atomization process is one of the main factors influencing the combustion performance [2]. One technical implementation for injection systems is the airblast atomizer. It creates a thin kerosene film on the inner wall of a cylinder called prefilmer. A parallel fast flowing air stream accelerates the liquid fuel which is supposed to disintegrate at the end of the prefilmer (atomizing lip).

Due to the limited computational resources it is difficult to simulate the whole atomization process in combination with the combustion in a single calculation in a reasonable time. Therefore, the primary formation process of the spray is often neglected in combustion simulations. Instead, droplet size distributions, which are measured downstream of the atomizer, are used as initial conditions [3–5] or even empirical correlations [6–10]. The disadvantage is that

those measurements normally run at lower pressure than the technical application due to the limited applicability of the measurement techniques to high pressure. However, the phenomenon called surface stripping (separation of droplets of the interface from a liquid film [11]), which gets important at high working pressure, changes the droplet size distribution. Therefore, the use of a droplet size distribution measured at low pressure in a simulation at higher pressure is not possible without uncertainties.

In [12] an energy equilibrium is used to derive a correlation for the generated Sauter mean diameter of the atomization of a liquid sheet produced by a flat-sheet airblast atomizer. The same procedure is used for the derivation of a correlation for the Sauter mean diameter of an atomized liquid jet generated by a plain-jet airblast atomizer. Based on the idea of the energy equilibrium a correlation for the Sauter mean diameter of an atomized liquid jet produced by an external-mixing twin-fluid atomizer is derived in [13]. In comparison to the work of Lefebvre [12], this correlation is not only fitted to experimental results at different pressure with the help of fit parameters, but also with the help of exponents.

In the presented work the energy equilibrium is adapted to a simplified planar prefilmer airblast atomizer. The proportionality factors of this correlation are determined with the help of numerical simulations of a three-dimensional multiphase flow. The results of the derived correlation are

Melanie Volz (melanie.volz@kit.edu), Dr. Peter Habisreuther, Prof. Dr. Nikolaos Zarzalis, Karlsruhe Institute of Technology, Engler-Bunte-Institute, Division of Combustion Technology, Engler-Bunte-Ring 1, 76131 Karlsruhe, Germany.

compared to a correlation from literature [10] that is based on experimental results at atmospheric conditions. In those experiments, amongst others, the air velocity, surface tension and liquid viscosity is changed to investigate the influence on the produced droplet size.

In this work it is shown that the newly derived correlation agrees well with the results from the numerical simulations, so that more reliable boundary conditions for combustion simulations can be gained with the help of the presented correlation.

2 Numerical Models

The CFD code interFoam of the OpenFOAM 2.1.1-package [14] is used in this work. The interface of two incompressible fluids (a gaseous and liquid phase) is calculated with the volume of fluid (VOF) method [15]. The interface is determined with the help of the liquid volume fraction α , which is the relation between the volume of a cell occupied by liquid, V_L , and the volume of the considered cell, V_{cell} :

$$\alpha = \frac{V_L}{V_{\text{cell}}} \quad (1)$$

where $\alpha = 0$ or $\alpha = 1$ indicates that a cell is completely filled with gaseous phase or liquid, respectively. In the interface region of the two fluids ($0 < \alpha < 1$), the density ρ and kinematic viscosity ν are weighted with α :

$$\begin{aligned} \rho &= \rho_L \alpha + \rho_G (1 - \alpha) \\ \nu &= \nu_L \alpha + \nu_G (1 - \alpha) \end{aligned} \quad (2)$$

where the index L denotes the liquid and the index G the gas phase.

The transport equation of α is:

$$\frac{\partial \alpha}{\partial t} + \frac{\partial(\alpha u_i)}{\partial x_i} + \frac{\partial}{\partial x_i} (u_{i,\text{rel}} \alpha (1 - \alpha)) = 0 \quad (3)$$

where t describes the time, u_i the velocity in x_i -direction and $u_{i,\text{rel}}$ the relative interface velocity [16]. The third term on the left hand side describes the artificial compression of the interface of the fluids to reduce the numerical diffusion.

In the Navier-Stokes equations an additional term is required in order to consider the pressure created by the surface tension σ_L with the help of the continuum surface force (CSF) model [17]:

$$\frac{\partial u_i}{\partial t} + \frac{\partial(u_i u_j)}{\partial x_j} = -\frac{1}{\rho} \frac{\partial p}{\partial x_i} + \nu \frac{\partial^2 u_i}{\partial x_j \partial x_j} + g_i + \frac{1}{\rho} \sigma_L \kappa \nabla \alpha \quad (4)$$

where κ denotes the curvature of the interface.

The turbulence is modeled with the k - ϵ turbulence model, which is adapted for two-phase flows. The volume of fluid method and the adapted k - ϵ turbulence model for two-phase flows are described in detail in [18].

3 Numerical Setup

The numerical setup is the same as in [18] and is shown in Fig. 1. The wedge separates the liquid and gas phase entry before the fluids interact on the prefilmer. The cubical cells of the computational grid have an edge size of $30 \mu\text{m}$ and are equidistantly distributed into the flow direction (y -axis).

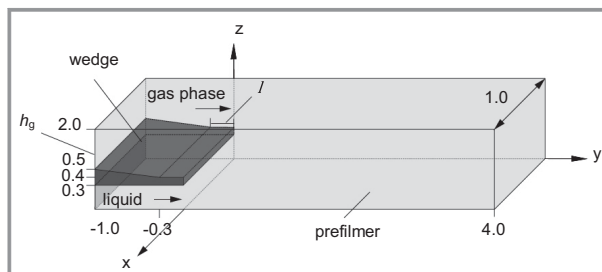


Figure 1. Computational domain (all dimensions in [mm]).

The operating conditions of the investigated case are listed in Tab.1. The gas properties are taken from REFPROP 8 [19]. The standard gas phase is air and the standard liquid is kerosene. The calculation of the kerosene properties are based on [20] for an ambient temperature of 20°C (density $\rho_L = 805.48 \text{ kg m}^{-3}$). A fully developed liquid velocity profile is used as boundary condition with a mean velocity of $v_L = 1 \text{ m s}^{-1}$. The air inlet velocity is varied in a range of 30 to 90 m s^{-1} . Additionally, the influence of the pressure is investigated between 2 and 12 bar. For the investigation of the influence of surface tension σ_L and gaseous kinematic viscosity ν_G these parameters are varied separately. Consequently, the properties of the liquid and gas phase chosen for some of the simulations do not correspond to realistic fluids.

In addition, the parameters are varied in such a way that the Weber number remains constant at 338, because it is reported in [11] that under those conditions the surface stripping, the separation of droplets from a liquid film, takes place. Thus, the influence of the Weber number and its capability to be used to predict the start of the formation of the first droplets on a film could be investigated. The Weber number is calculated with the height of the liquid channel $h = 0.3 \text{ mm}$ as characteristic length [11]:

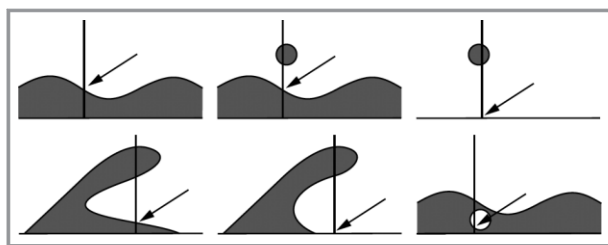
$$\text{We} = \frac{\rho_G v_G^2 h}{\sigma_L} \quad (5)$$

4 Analysis Methods

The complex surface topology existing of breaking waves, ligaments and droplets on the film initiated by the fast moving gas flow is shown in Fig. 2. The arrows mark the definition of the film thickness. As a consequence of this definition, droplets above the film and the upper part of breaking waves are not considered.

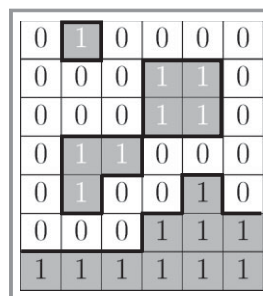
Table 1. Operating conditions used in the simulations.

Case	v_G [m s ⁻¹]	p [bar]	ρ_G [kg m ⁻³]	ν_G [mm ² s ⁻¹]	ν_L [mm ² s ⁻¹]	σ_L [10 ⁻³ N m ⁻¹]	We [-]
1	60	6	7.14	2.57	1.82	22.8	338
2	30	6	7.14	2.57	1.82	22.8	84
3	40	6	7.14	2.57	1.82	22.8	150
4	90	6	7.14	2.57	1.82	22.8	760
5	60	2	2.38	7.68	1.82	22.8	112
6	60	3	3.57	5.12	1.82	22.8	169
7	60	4	4.76	3.84	1.82	22.8	225
8	60	6	7.14	2.57	1.82	9.8	790
9	60	6	7.14	2.57	1.82	49.2	157
10	90	6	7.14	2.57	1.82	9.8	1776
11	90	6	7.14	2.57	1.82	49.2	353
12	60	6	7.14	1.285	1.82	22.8	338
13	60	6	7.14	5.14	1.82	22.8	338
14	60	3	3.57	5.12	1.82	11.4	338
15	42.4	6	7.14	2.57	1.82	11.4	338
16	42.4	12	14.29	1.29	1.82	22.8	338

**Figure 2.** Determination of the film thickness (liquid is marked with gray color).

550 time steps with a time difference of 10^{-4} s have been analyzed for each case of Tab. 1. The droplets and ligaments consist of those cells that are filled with liquid ($\alpha \geq 0.5$) and are not considered in the determination of the film thickness as illustrated in Fig. 3. In the shown two-dimensional plane the white cells mark the gaseous phase ($\alpha < 0.5$) and the gray cells the liquid phase ($\alpha \geq 0.5$). The gray cells with a black number 1 represent the liquid film, while droplets are represented by gray cells with a white number 1. In the two-dimensional case a droplet is a region of cells that are connected with the edges of the neighbor cells and filled with liquid ($\alpha \geq 0.5$). Therefore, three droplets are shown in Fig. 3. If two neighbor cells are only connected with one corner of those cells, it is assumed that they belong to two different droplets.

In a three-dimensional case the cells have to be connected with a whole area of two neighboring cells so that they can

**Figure 3.** Determination of droplet volumes.

form one droplet. If they are only connected with the edges, it is assumed that they belong to two different droplets. The volume V_{dr} of one droplet is the sum of the volume of the cells which form the droplet. Using the simplification that every droplet is spherical, its diameter d_{dr} is calculated with:

$$d_{dr} = \left(\frac{6V_{dr}}{\pi} \right)^{1/3} \quad (6)$$

This calculation step is performed for every droplet at every considered time step on the prefilmer in order to describe the whole emerging droplet collective.

The Sauter mean diameter d_{SMD} is the diameter of a homogeneous spray with the same volume to surface ratio as the original droplet collective. Therefore, the determination of this diameter based on the individually calculated droplet diameters provides one value for the comparison of the average size of droplets at different boundary conditions:

$$d_{\text{SMD}} = \frac{\sum_{n=1}^{N_{\text{dr}}} d_{\text{dr},n}^3}{\sum_{n=1}^{N_{\text{dr}}} d_{\text{dr},n}^2} \quad (7)$$

The number of all considered droplets is N_{dr} .

5 Derivation of a Correlation Based on Energy Balance

Based on the above mentioned simulations a correlation for the Sauter mean diameter d_{SMD} is derived in a similar way as described in [12, 19]. The main idea of the derivation is that energy is necessary to increase the surface of a liquid phase when waves and droplets are formed against the surface tension of the liquid. The energy necessary for this process is transferred from the gas phase to the liquid phase. Equating both energies results in the correlation of the Sauter mean diameter.

In [13] a liquid jet is atomized and it is assumed that the kinetic energy of the gas phase is used for the atomization of the cylindrical liquid jet. In this work a thin, shear-driven liquid film is atomized. Therefore, the energy which is transferred from the gas phase to the liquid is the shear stress of the gas phase:

$$\dot{E} = \tau \dot{V}_L = \tau \frac{\dot{m}_L}{\rho_L} \quad (8)$$

with \dot{V}_L being the volume flow of the liquid film, which is the ratio of the mass flow of liquid \dot{m}_L to the density of the liquid ρ_L . The acceleration of the film due to the shear stress depends on the volume flow of the liquid. The probability for the formation of ligaments and droplets increases with higher acceleration of the film.

The shear stress of the gas phase τ is given by:

$$\tau = \nu_G \rho_G \frac{\partial v_G}{\partial z} \quad (9)$$

where $\partial v_G / \partial z$ stands for the velocity gradient of the gas phase. For its calculation the assumption is made that the liquid velocity is negligibly small. This assumption is justified by the fact that the velocity of the gas phase is much higher than the liquid velocity in the cases considered. The height of the relevant velocity gradient can be expressed using the laminar boundary thickness δ_{lam} of the interface of both fluids:

$$\tau = \nu_G \rho_G \frac{\nu_G}{\delta_{\text{lam}}} \quad (10)$$

Following [20] the laminar boundary thickness is expressed in terms of:

$$\delta_{\text{lam}} = \frac{0.5l}{\text{Re}_G^{0.5}} \quad (11)$$

where l represents the length of the last, horizontal part of the wedge ($l = 0.3 \text{ mm}$). There the flow cross-section is constant and the velocity profile of the gas phase can develop undisturbed. The Reynolds number Re_G is calculated as follows:

$$\text{Re}_G = \frac{\nu_G h_G}{\nu_G} \quad (12)$$

with the characteristic length h_G being the height of the domain in which the gas phase enters it ($h_G = 1.5 \text{ mm}$).

Using Eq. (9) the energy flow caused by the shear stress of the gas phase (Eq. (8)) is:

$$\dot{E}_\tau = \nu_G \rho_G \frac{\nu_G}{\delta_{\text{lam}}} \frac{\dot{m}_L}{\rho_L} \quad (13)$$

The energy flow which is necessary for the enlargement of the surface of the liquid film is:

$$\dot{E}_\sigma = \sigma_L \Delta \dot{A} = \sigma_L (\dot{A}_{\text{dr}} - \dot{A}_{\text{L,s}}) \quad (14)$$

where $\Delta \dot{A}$ is the increase of the surface per second due to the formation of droplets.

It is assumed that all formed droplets have the same diameter, the Sauter mean diameter d_{SMD} . Therefore, the surface flow of produced droplets is:

$$\dot{A}_{\text{dr}} = \dot{n} \pi d_{\text{SMD}}^2 \quad (15)$$

with \dot{n} being the number of produced droplets per second. The mass flow of droplets is:

$$\dot{m}_{\text{dr}} = \dot{n} \rho_L \frac{\pi}{6} d_{\text{SMD}}^3 \quad (16)$$

In order to eliminate \dot{n} from Eq. (15), Eq. (16) is used leading to:

$$\dot{A}_{\text{dr}} = \frac{6\dot{m}_{\text{dr}}}{\rho_L d_{\text{SMD}}} \quad (17)$$

In the current case the prefilmer is not long enough to atomize the liquid completely. Therefore, the amount of liquid which is actually separated from the film in form of ligaments and droplets is assumed to be a fixed part f_{part} of the whole liquid surface flow:

$$\dot{A}_{\text{dr}} = f_{\text{part}} \frac{6\dot{m}_L}{\rho_L d_{\text{SMD}}} \quad (18)$$

The flow of the free surface of the liquid film is:

$$\dot{A}_{\text{L,s}} = \frac{\dot{m}_L}{\rho_L h_L} \quad (19)$$

with h_L being the height of the liquid film. In the current case the initial film height $h(y = 0) = h_L = 300 \mu\text{m}$ is used. Therefore, Eq. (14) can be written as

$$\dot{E}_\sigma = \sigma_L \Delta \dot{A} = \sigma_L \left(\frac{6f_{\text{part}} \dot{m}_L}{\rho_L d_{\text{SMD}}} - \frac{\dot{m}_L}{\rho_L h_L} \right) \quad (20)$$

The basic idea of this procedure is that both energy flows (Eq. (13) and (20)) are proportional:

$$\dot{E}_\tau \sim \dot{E}_\sigma \quad (21)$$

$$v_G \rho_G \frac{v_G}{\delta_{\text{lam}}} \frac{\dot{m}_L}{\rho_L} \sim \sigma_L \frac{\dot{m}_L}{\rho_L} \left(\frac{6f_{\text{part}}}{d_{\text{SMD}}} - \frac{1}{h_L} \right) \quad (22)$$

Solving Eq. (22) for d_{SMD} and including the proportionality constant f_{lam} leads to:

$$d_{\text{SMD}} = \frac{6f_{\text{part}}}{\frac{1}{h_L} - \frac{\rho_G v_G v_G}{f_{\text{lam}} \delta_{\text{lam}} \sigma_L}} \quad (23)$$

The two unknown constants are determined using results of the numerical simulations together with error minimization by the least squares method to $f_{\text{lam}} = 2.23$ and $f_{\text{part}} = 0.34$. This result can be interpreted that 34% of the liquid is atomized on its way on the prefilmer. The root mean square of the least squares method is 0.0002.

6 Results and Discussion

In order to validate the derived correlation (23) the Sauter mean diameter calculated from this correlation is compared to results using a correlation from literature [10] that is based on experimental data:

$$d_{\text{SMD}} = l_c \left(1 + \frac{\dot{m}_L}{\dot{m}_G} \right) \left(f_1 \left(\frac{\sigma_L}{\rho_G v_G^2 l} \right)^{0.6} \left(\frac{\rho_L}{\rho_G} \right)^{0.1} + f_2 \left(\frac{v_L^2}{\sigma_L \rho_L L} \right)^{0.5} \right) \quad (24)$$

where the characteristic length l_c is the initial height of the liquid film ($l_c = 300 \mu\text{m}$) and l is the length of the prefilmer ($l = 4 \text{ mm}$). The factors $f_1 = 44.78$ and $f_2 = 1.02$ have been determined with the least squares method to minimize the difference between the results of Eq. (24) and the simulations. The method results in a root mean square error of 0.0004.

This correlation is used for example in [21] and [23] for the comparison with experimental data. It is shown that the correlation can predict the experimental results, but more often it fails.

For comparison the Sauter mean diameter of the numerical simulations (filled symbols) are plotted together with the Sauter mean diameter calculated with the correlation (23) (empty symbols and marked with "corr") in Fig. 4. The

numbers in the legends correspond to the case number of the parameter variation given in Tab. 1. For a better overview, the cases are ordered in such a way that the varied parameter increases from top to bottom in the legend. In addition, the results from the empirical correlation Eq. (24) are included in Fig. 4 and marked with "lit".

Fig. 4a shows that the Sauter mean diameter from both, the simulations and from the derived correlation Eq. (23), agree qualitatively and quantitatively well with each other. The correlation from literature (Eq. (24)) instead captures only the tendencies. For high gas velocity the deviations from the results of the correlation Eq. (23) is over ten times smaller than the deviation of correlation Eq. (24) from the simulations.

As illustrated in Fig. 4b the dependency of the working pressures is correctly described from the results of the correlation derived in this work (see Eq. (23)). The following comparison emphasizes the important influence of the gas velocity on the atomization process as it is reported in literature [8, 10]: by an increase of the working pressure of a factor of 2 (from 3 to 6 bar), the Sauter mean diameter of the correlation decreases by approximately 13% and the Sauter mean diameter of the simulation by approximately 28%. Increase of the gas velocity by a factor of 2 (from 30 to 60 m s^{-1}) results in a decrease of the Sauter mean diameter of the correlation by approximately 32% and for the simulation by approximately 40%. The correlation from the literature Eq. (24) captures this tendency, but the difference between its results and the data from the simulation increases for lower (2 bar) and higher pressure (6 bar).

Fig. 4c shows the comparison of the results of the Sauter mean diameter by a variation of the surface tension for the gas velocity of 60 and 90 m s^{-1} . The same tendency is observed for the simulation and the derived correlation Eq. (23): the Sauter mean diameter increases with higher surface tension. Furthermore, the Sauter mean diameter decreases for a constant surface tension but increasing velocity of the gas phase. The correlation from the literature Eq. (24) again is able to capture the tendencies, but underestimates the results.

The influence of the kinematic viscosity of the gaseous phase on the Sauter mean diameter is shown in Fig. 4d. The diameter slightly decreases with higher kinematic viscosity. The derived correlation from the literature Eq. (24) predicts a constant Sauter mean diameter because Eq. (24) does not depend on the kinematic viscosity.

Fig. 4e shows the Sauter mean diameter in dependency of the working pressure for a constant Weber number $We = 338$. As a result of the comparison it can be stated that the Weber number is not sufficient to consider all the relevant effects of the simulated atomization process (as it is also reported in [21]). This conclusion is based on the fact that different diameters are observed by the variation of the parameters of the constant Weber number. The maximum deviation of the Sauter mean diameter from the simulation is 18% and from Eq. (23) 23%. The variation of the results

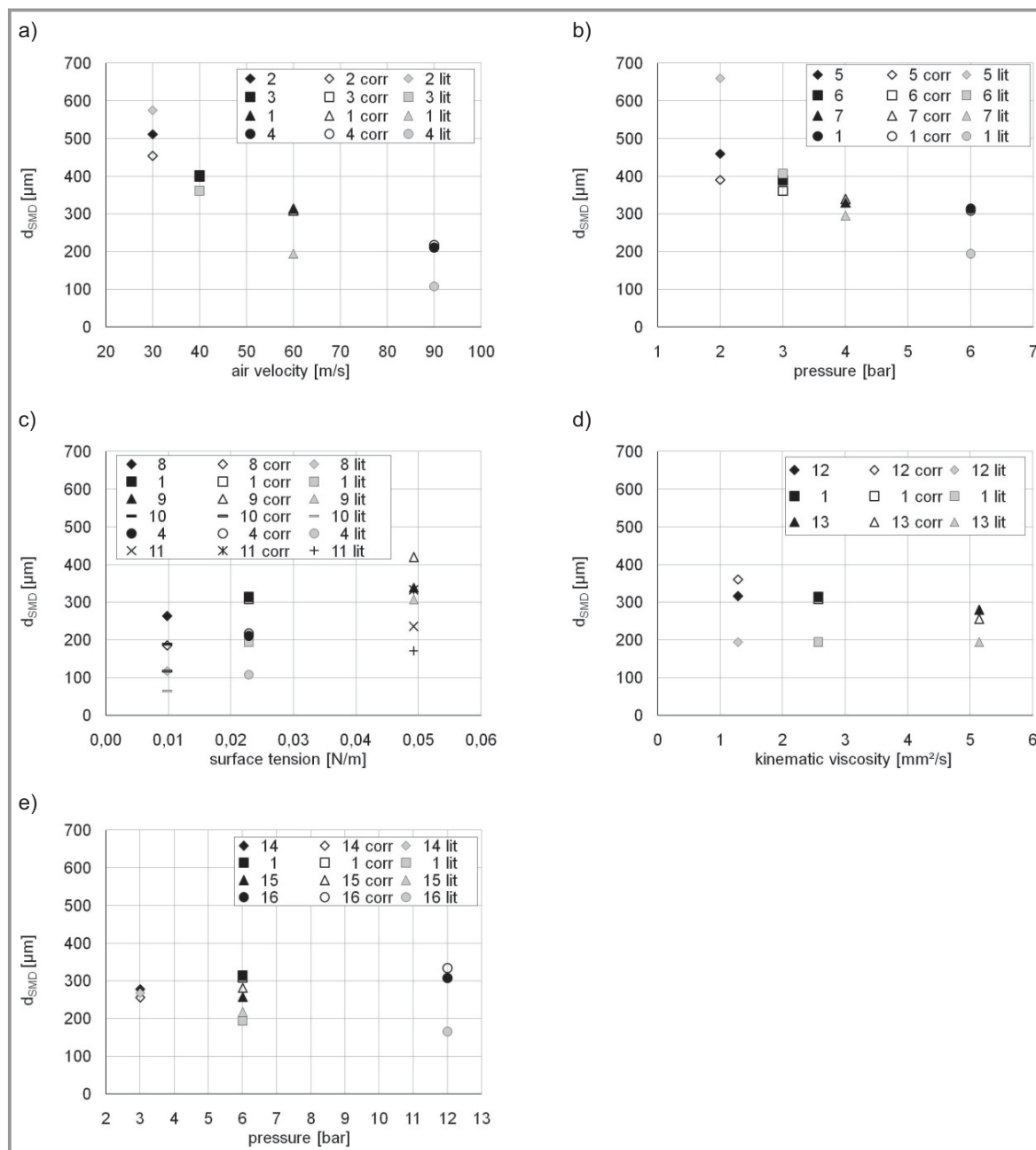


Figure 4. Comparison of the numerical results with the correlations. a) Variation of gas velocity; b) variation of working pressure; c) variation of surface tension; d) variation of gaseous kinematic viscosity; e) constant Weber number $We = 338$.

can also be used to show the influence of different parameters. At a constant surface tension (case 16 and 17, 1 and 18) the Sauter mean diameter increases by a decrease of gas velocity and an increase of working pressure. Consequently smaller droplets are created by higher gas velocity. The correlation from the literature Eq. (24) instead predicts that the Sauter mean diameter decreases with increasing pressure.

Summarizing the above shown results the Sauter mean diameter of the correlations are plotted against the Sauter mean diameter from the numerical simulations (Fig. 5). The

overview depicts the improved capability of the newly derived correlation to resemble the Sauter mean diameter from the detailed simulations. The averaged difference between the Sauter mean diameter of the simulation and the derived correlation Eq. (23) is $41 \mu\text{m}$ whereas the averaged difference between the Sauter mean diameter of the simulation and of the correlation from the literature Eq. (24) is $79 \mu\text{m}$. The constant deviation of the Sauter mean diameter of the simulation is $\pm 25\%$ (dotted line), while the deviation of the correlation from the literature is $\pm 50\%$ (dashed line).

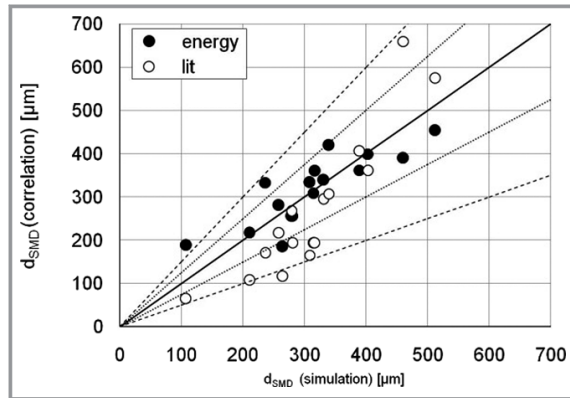


Figure 5. Comparison of the Sauter mean diameter of the correlations.

7 Conclusion

A broad range of parameters influencing the Sauter mean diameter of droplets which are separated from a liquid film on a prefilmer of a simplified airblast atomizer are simulated. The results show that the Sauter mean diameter depends mainly on the gas velocity. These results are compared with a correlation that has been derived considering the equilibrium of the energy which is necessary to increase a liquid surface and the energy which is transferred by the shear stress from the gas to the liquid phase, and a correlation from literature. Qualitatively and quantitatively there is a good agreement between the Sauter mean diameter from the correlation derived in the current work and from numerical simulations. The literature correlation instead is able to capture most tendencies, but fails when reproducing the absolute values.

The authors gratefully acknowledge the financial support by the federal state Baden-Württemberg, Germany through the project “Future Offensive IV: Innovation and Excellence“. The computation time has been kindly provided by the Steinbuch Centre for Computing of the Karlsruhe Institute of Technology.

Symbols used

\dot{A}	$[\text{m}^2\text{s}^{-1}]$	surface flow
d	$[\text{m}]$	diameter
d_{SMD}	$[\text{m}]$	Sauter mean diameter
\dot{E}	$[\text{J s}^{-1}]$	energy flow
f	$[-]$	factor
g_i	$[\text{m s}^{-2}]$	gravitational component in i -direction
h	$[\text{m}]$	height
l	$[\text{m}]$	length
\dot{m}	$[\text{kg s}^{-1}]$	mass flow

\dot{n}	$[\text{s}^{-1}]$	number per second
p	$[\text{N m}^{-2}]$	working pressure
Re	$[-]$	Reynolds number
u, v, w	$[\text{m s}^{-1}]$	velocity components in x, y, z -direction
\dot{V}	$[\text{m}^3\text{s}^{-1}]$	volume flow
We	$[-]$	Weber number
x, y, z	$[\text{m}]$	Cartesian coordinates

Greek symbols

α	$[-]$	liquid volume fraction
κ	$[\text{m}^{-1}]$	curvature
δ_{lam}	$[\text{m}]$	laminar boundary thickness
ν	$[\text{m}^2\text{s}^{-1}]$	kinematic viscosity
ρ	$[\text{kg m}^{-3}]$	density
σ	$[\text{N m}^{-1}]$	surface tension
τ	$[\text{N m}^{-2}]$	shear stress

Subscripts


c	characteristic
cell	mesh cell
G	gas phase
i	running index ($i = 1, 2, 3$)
j	running index ($j = 1, 2, 3$)
dr	droplet
L	liquid
lam	laminar
part	partial
s	surface

References


- [1] A. Lefebvre, *Gas Turbine Combustion*, 2nd ed. Taylor and Francis, Philadelphia, PA **1998**.
- [2] A. Lefebvre, D. Miller, *The development of an air blast atomizer for gas turbine application*, CoA. Report AERO No. 193, College of Aeronautics Cranfield, **1966**.
- [3] S. Apte, K. Mahesh, P. Moin, *Proc. Combust. Inst.* **2009**, 32 (2), 2247.
- [4] M. Sanjosé, J. Senoner, F. Jaegle, B. Cuenot, S. Moreau, T. Poinsot, *Int. J. Multiphase Flow* **2011**, 37 (5), 514.
- [5] J. Keller, M. Gebretsadik, P. Habisreuther, F. Turrini, N. Zarzalis, D. Trimis, *Int. J. Multiph. Flow* **2015**, 75, 144.
- [6] A. Rizkalla, A. Lefebvre, *J. Fluids Eng.* **1975**, 97 (3), 316. DOI: 10.1115/1.3447309
- [7] A. Rizkalla, A. Lefebvre, *J. Eng. Power* **1975**, 97 (2), 173. DOI: 10.1115/1.3445951
- [8] G. Lorenzetto, A. Lefebvre, *AIAA J.* **1977**, 15 (7), 1006.
- [9] N. Rizk, A. Lefebvre, *J. Eng. Gas Turbines Power* **1984**, 106 (3), 634. DOI: 10.1115/1.3239617
- [10] M. El-Shanawany, A. Lefebvre, *J. Energy* **1980**, 4 (4), 184.
- [11] U. Bhayaraju, *Ph.D. Thesis*, Technischen Universität Darmstadt **2007**.
- [12] A. Lefebvre, *J. Eng. Gas Turbines Power* **1992**, 114 (1), 89. DOI: 10.1115/1.2906311

- [13] T. Jakobs, N. Djordjevic, A. Sanger, N. Zarzalis, T. Kolb, *Atomization Sprays* **2015**, 25 (12), 1081.
- [14] OpenFOAM User Guide, OpenFOAM-Foundation, London **2011**.
- [15] C. Hirt, B. Nichols, *J. Comput. Phys.* **1981**, 39 (1), 201. DOI: 0021.9991/81/010201
- [16] H. Weller, *A New Approach to VOF-based Interface Capturing Methods for Incompressible and Compressible Flow*, Caversham **2008**.
- [17] J. Brackbill, D. Kothe, *J. Comput. Phys.* **1992**, 100 (2), 335.
- [18] M. Volz, L. Nittel, P. Habisreuther, N. Zarzalis, *Chem. Ing. Tech.* **2016**, 88 (1 – 2), 192. DOI: 10.1002/cite.201500011
- [19] E. Lemmon, M. Huber, M. McLinden. *NIST Standard Reference Database 23: Reference Fluid Thermodynamic and Transport Properties-REFPROP*, Version 9.1, National Institute of Standards and Technology, Standard Reference Data Program, Gaithersburg, **2013**.
- [20] M. Rachner, *Die Stoffeigenschaften von Kerosin Jet A-1*, Deutsches Zentrum fur Luft- und Raumfahrt e.V., Koln **1998**.
- [21] S. Gepperth, R. Koch, H. Bauer, in *Proc. of ASME Turbo Expo*, San Antonio, TX **2013**.
- [22] H. Schlichting, *Grenzschicht-Theorie*, 10th ed., Springer, Berlin **2006**.
- [23] C. Wollgarten, M. Gebretsadik, N. Zarzalis, T. Fabio, O. Sara, P. Di Martino, in *Proc. of ASME Turbo Expo*, San Antonio, TX **2013**.

Neugierig?



Erlebnis Wissenschaft




KARIN BODEWITS, ANDREA HAUKE,
PHILIPP GRAMLICH

**Karrierefuhrer
fur Naturwissenschaftlerinnen**
Erfolgreich im Berufsleben

ISBN: 978-3-527-33839-9
Oktober 2015 328 S. mit 1 Tab.
Broschur € 29,90

NEU



In Deutschland schlieen inzwischen ebenso viele Frauen wie Manner ein naturwissenschaftliches Studium ab. Welche Karrieremoglichkeiten stehen ihnen offen?

Die Autoren zeigen in diesem etwas anderen Karrierefuhrer, wie Naturwissenschaftlerinnen die Widrigkeiten des Berufseinstiegs meistern und schon wahrend des Studiums die Weichen richtig stellen konnen, um im Berufsleben zu bestehen.

Der lockere und humorvolle Stil macht das Buch zu einem sympathischen Begleiter durch das Berufsleben, den man bzw. frau nicht mehr missen mochte.

e
Auch als
E-Book unter:
www.wiley-vch.de/ebooks/

www.wiley-vch.de/sachbuch

SB_Bodewi_175x125_bw_bu

Irtrum und Preisanderungen vorbehalten. Stand der Daten: August 2015.

Wiley-VCH • Postfach 10 11 61 • D-69451 Weinheim
Tel. +49 (0)6201-606400 • e-mail: service@wiley-vch.de

WILEY-VCH